



**HAL**  
open science

## A strategy for geostationary positioning with GNSS signals

Benjamin Chibout, Christophe Macabiau, Anne-Christine Escher, Lionel Ries,  
Jean-Luc Issler, Stéphane Corazza

► **To cite this version:**

Benjamin Chibout, Christophe Macabiau, Anne-Christine Escher, Lionel Ries, Jean-Luc Issler, et al..  
A strategy for geostationary positioning with GNSS signals. ION GNSS 2007, 20th International  
Technical Meeting of the Satellite Division of The Institute of Navigation, Sep 2007, Fort Worth,  
United States. pp 2388 - 2400. hal-01022133

**HAL Id: hal-01022133**

**<https://enac.hal.science/hal-01022133>**

Submitted on 20 Nov 2014

**HAL** is a multi-disciplinary open access archive for the deposit and dissemination of scientific research documents, whether they are published or not. The documents may come from teaching and research institutions in France or abroad, or from public or private research centers.

L'archive ouverte pluridisciplinaire **HAL**, est destinée au dépôt et à la diffusion de documents scientifiques de niveau recherche, publiés ou non, émanant des établissements d'enseignement et de recherche français ou étrangers, des laboratoires publics ou privés.

# A strategy for Geostationary Positioning with GNSS Signals

B.Chibout, C.Macabiau, A-C.Escher, *Ecole Nationale de l'Aviation Civile/Tesa*  
L.Ries, J-L.Issler, *CNES*  
S.Corrazza, *ThalesAleniaSpace*

## BIOGRAPHY

Benjamin Chibout is a Ph.D. student in the field of GPS space application in the signal processing lab of the Ecole Nationale de l'Aviation Civile (ENAC) in Toulouse, France. He graduated in 2004 as an electronics engineer from the ENAC, and received the same year his Master research degree in signal processing.

Christophe Macabiau graduated as an electronics engineer in 1992 from ENAC in Toulouse, France. Since 1994, he has been working on the application of satellite navigation techniques to civil aviation. He received his Ph.D. in 1997 and has been in charge of the signal processing lab of the ENAC since 2000.

Anne-Christine ESCHER graduated as an electronics engineer in 1999 from the ENAC in Toulouse, France. Since 2002, she has been working as an associated researcher in the signal processing lab of the ENAC. She received her Ph.D. in 2003.

Lionel Ries is a navigation engineer in the "Transmission Techniques and Signal Processing Department", at CNES since June 2000. He is responsible of research activities on GNSS2 signals, including BOC modulations and modernised GPS signals (L2C & L5). He graduated from the Ecole Polytechnique de Bruxelles, at Brussels Free University (Belgium) and then specialized in space telecommunications systems at Supaero (ENSAE), in Toulouse (France).

Jean-Luc Issler is head of the Transmission Techniques and signal processing department of CNES, whose main tasks are signal processing, air interfaces and equipments in Radionavigation, TT&C, propagation and spectrum survey. He is involved in the development of several spaceborne receivers in Europe, as well as in studies on the European RadioNavigation projects, like GALILEO and the Pseudolite Network. With DRAST and DGA, he represents France in the GALILEO Signal Task Force of the European Commission. With Lionel Ries and Laurent Lestarquit, he received the astronautic prize 2004 of the

French Aeronautical and Astronautical Association (AAAF) for his work on Galileo signal definition.

Stéphane Corazza is a research and development engineer in Thales Alenia Space company. He has experience in GPS and Galileo receivers design, digital signal processing suited to radiocommunications and satellite navigation, ASIC and FPGA development for satellite digital payloads. He has received engineering degree in Electronics and Telecommunication in the National Institute of Applied Sciences (INSA - Lyon, France, 1994).

## ABSTRACT

GNSS signal processing for a receiver in a geostationary environment is more difficult than for a classical receiver on Earth in normal conditions. There are numerous differences between the GNSS signals that an Earth user receives and the signals that a geostationary satellite receives. The specific and main characteristics of the GNSS signal received by a geostationary satellite are the following: high C/No values only for ray tangential to the earth, with C/No more frequently between 20dBHz and 24dBHz, very important Doppler values (+/-15kHz), and poor Dilution Of Precision factor (usually higher than 5). To cope with these particular constraints we propose to elaborate a GPS signal processing strategy that has the particularity to be autonomous, that is the receiver does not use "aiding data" downloaded from Earth to compute its position. In that case, the complexity of the receiver as well as its cost is lowered. Its integration in the satellite payload is eased too. The geostationary receiver position is computed along the day mainly through an acquisition snapshot process and an orbital filter.

As the Doppler range is too large to be processed, as a preliminary step of the strategy, we reduce the Doppler uncertainty by computing the GPS satellite position thanks to almanacs data previously demodulated. This preliminary step is investigated in the first part of the paper. To be able to process enough GPS signals all along the day, with a geometry as good as possible but still limited due to the situation, we implement an acquisition

method that is able to cope with C/N0 signal values as low as 20 dBHz. Thus, three techniques have been studied and evaluated: the FFT acquisition method, the Half Bit method and the last one is called the Double Block Zero Padding method. Yet, in parallel to that, we have to ensure that the receiver may be autonomous in that it is able to know enough valid ephemeris data from visible satellites to compute its position thanks to the pseudorange measurements. Indeed, the position of the GPS satellites computed thanks to almanacs data is not enough accurate to compute the geostationary satellite receiver position. It has been shown in [2] that the data demodulation threshold must be lowered down to 25 dBHz to be sure to see at least four GPS satellites with valid ephemeris data at any time during the day.

Once we have fixed the demodulation threshold to ensure the autonomy of the receiver, the position is computed through acquisition snapshots. But the position estimate obtained after the acquisition process depends on the accuracy of the peak detection and so, it depends on the sampling rate. The results obtained by using the three above mentioned acquisition schemes do not lead to an accurate position calculation mainly because of the geometry of the acquired GPS satellites. That is why we propose to implement a peak extrapolation technique to improve the accuracy of the peak detection and thus, the accuracy of the estimated pseudorange measurement. Last, in order to improve the position estimate accuracy, we propose to implement an orbital filter to be coupled with the GNSS measurements elaborated at the output of the acquisition process, that takes into account the main forces which drive the movement of a geostationary satellite. The performance of this filter is analyzed in the last part of the paper. The aim of the paper is to present and assess the performance of the global strategy outlined above to process GPS signals with a receiver onboard a geostationary satellite based on the former characteristics. This paper is organized as follows: first, the constraints due to the geostationary orbit are briefly reminded, then the strategy is presented in a second part, particularly we stress the means to have an autonomous receiver. A third part is dedicated to the three acquisition techniques and their performances in term of position accuracy and availability are presented. A peak acquisition extrapolation is also detailed. In the last part, a Kalman filter using a simple force model to describe the satellite motion is studied to improve the accuracy of the navigation solution. The computational cost of the strategy is also investigated.

## INTRODUCTION

There is a growing interest in achieving geostationary satellites localization by using GNSS signals. However, we recall the GPS signal received in a geostationary orbit is somewhat different from the signal that a classic earth user can encounter. The specific and main characteristics

of the signal received by a geostationary satellite are the following: the C/No values are spread around 15dBHz-25dBHz and roughly go up to 45dBHz; the Doppler values are very important (+/-15kHz), and the Dilution Of Precision factors are usually higher than 5.

A GNSS receiver onboard a geostationary satellite will have to deal with these specific constraints. Several acquisition strategies can be used to cope with these constraints and to produce an accurate position. Our aim in this work is to use acquisition techniques which work in a global autonomous acquisition strategy with a minimum computational cost to save energy. So the receiver does not use any "aiding data", such as GPS ephemeris or almanacs uploaded from the earth. Then, the complexity, the cost and the adaptability of the receiver is lowered, which is consistent with low energy consumption and simple integration within the payload. With these operating constraints, we have studied three different acquisition techniques to achieve the positioning and a Kalman filter to improve the accuracy of the calculated position.

The first part of this paper recalls the characteristics of the GPS signal when processing it on a geostationary orbit. The problems we face in the geostationary orbit to develop an autonomous signal processing are also presented. The next part details the solutions used to get rid of these problems; notably a solution to increase the number of GPS satellites with valid ephemeris the receiver can acquire is depicted. It also shows the developed strategy to reduce the number of operation the receiver carries out along the day.

The third part of this paper briefly presents three different acquisition techniques used to compute the geostationary satellite position: the first one is the classic FFT acquisition method, the second one is called the Half Bit method and the last one is called the Double Block Zero Padding method. The results over an entire day are presented with a classic least square estimation to estimate the position. A peak acquisition extrapolation technique is proposed to improve the accuracy of the estimated delay whose resolution is limited by the sampling frequency. The accuracy of the GEO satellite position is then improved.

The last part of the study proposes a Kalman filter to improve the accuracy of the position solution. The Kalman filter uses a simple force model to describe the geostationary satellite motion. Finally, the computational cost of the three acquisition techniques and the Kalman Filter are presented

## GPS SIGNAL CHARACTERISTICS FOR A GEOSTATIONARY ORBIT RECEIVER

The conditions for GPS signal processing are not as optimal for a GEO receiver as for an earth-based receiver. As depicted in figure 1, the GEO satellites are higher above the Earth than the GPS constellation orbit. Then,

for most of the time, the GPS antenna does not point in the direction of the GEO satellite antenna.

Let us denote zone 1 the area covered by the main lobe of the GPS antenna and zone 2 the area covered by the side lobe of the GPS antenna. Due to the directivity of the GPS antenna and the GEO receiver antenna, the received signal strength quickly decreases if the GPS signal is not emitted through the main lobe of the GPS antenna. Thus, the signals have more power when they are emitted by satellites in zone 1, at the opposite of the GEO satellite toward the earth. But, at each epoch, the number of GPS satellites located in this area is not large and the minimum of four satellites required to compute a position measurement is not met. The GEO only see 3 satellites for less than 60% of the time in this case and it is not sufficient to compute its position.

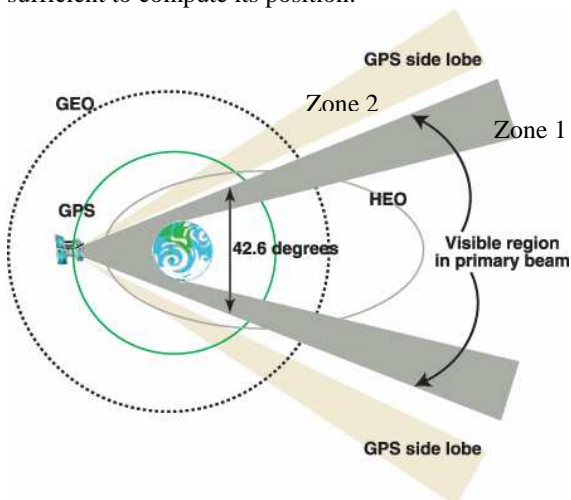


**Figure 1: Geostationary satellite visibility**

Besides, as in [1], the delay introduced by the crossing of the ionosphere for a signal tangent to the earth can fluctuate a lot and the delay can be as important as more than 100m. To protect ourselves from such a bias, we consider an earth masking for the following of the study, i.e we assume that the masking radius of the earth is the normal radius plus 1000km which stands for the ionosphere layer. The signals coming from that direction are not considered and thus, the number of “visible” satellites is lowered.

So, in order to increase the number of visible satellites as well as their visibility duration, signals emitted through side lobes of the GPS antenna, that is from zone 2, are considered. The received signal strength becomes far lower in this case while the elevation of the GPS satellite decreases. With the assumptions made in [1] (notably the GEO and GPS antenna gain pattern), the C/No of the received signals depending on the elevation of the GPS satellite towards the GEO is computed as illustrated in figure 2. The noise power density is set to -201dBHz.

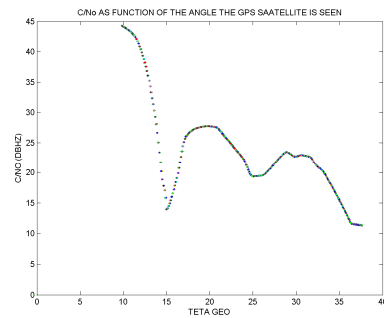


**Figure 2: Global C/No from the receiver point of view with GPS (L1) satellites,  $C/No=f(\frac{\pi}{2} - \text{elevation})$**

Teta GEO is the off-boresight angle of the GEO antenna. The figure 2 shows that the C/No ranges from 45 dBHz to less than 15 dBHz when considering the side lobes signals. The signal strength is weaker than for an Earth user in normal conditions. Most of the received signals have strength between 20 and 27 dBHz. So, to benefit from extra measurements, the acquisition techniques will have to work at least down to these values. In this case, it is a trade off between the low signal levels and the gain in the visibility duration of the GPS satellites. The figure 3 depicts the number of satellites the GEO satellite can see with a C/No higher than 20 dBHz and 25 dBHz. The visibility is computed for the geostationary satellite Artemis which is one of the EGNOS satellites.

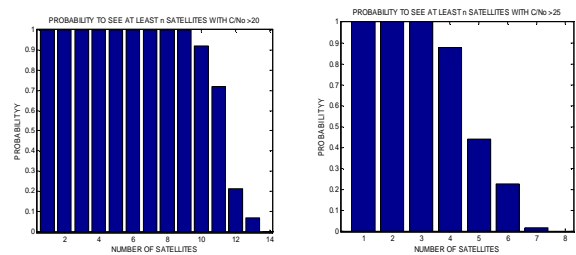


**Figure 3: Probability to see at least N satellites with  $C/No > 20$  dBHz (left) and  $C/No > 25$  dBHz (right)**

By processing signals down to 20 dBHz, 9 satellites are always visible and more than 12 are visible for more than 50% of the time. So, the receiver should be able to compute a point position. We note that the number of visible satellites significantly decreases when we want signals with a C/No higher than 25dBHz. In this case, it is possible to see 3 satellites at any time.

In addition to the global visibility problem, the period where each GPS satellite signal is received with a C/No higher than the data demodulation threshold (DDT) is a problem. Indeed, the signal of each GPS satellite is strong (i.e above the DDT) only for short periods and these periods can be spaced by several hours as it is depicted by figure 4.

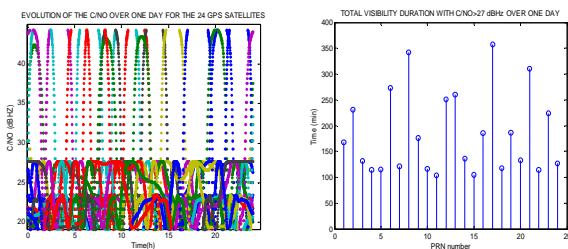


**Figure 4: Evolution of the C/N<sub>0</sub> , C/N<sub>0</sub>=f(time) (left) and duration of the C/N<sub>0</sub>>27dBHz (right) for the 24 GPS satellites over one day**

The usual DDT is set to 27dBHz for L1 C/A. The corresponding BER is  $6.10^{-6}$ . The duration for each GPS satellite where their C/N<sub>0</sub> is above this value is not long. The sum of the visibility intervals is within 100-200 minutes for most of the GPS PRN as shown in figure 4, where the total observation time is one day (1440 minutes).

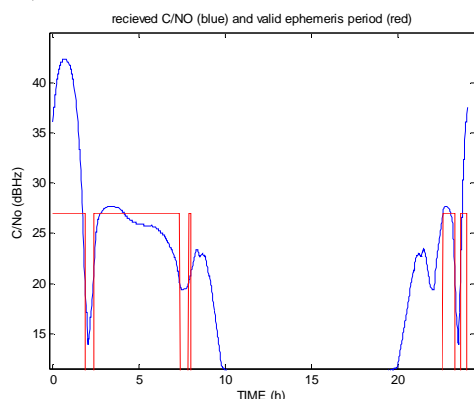


**Figure 5: Received C/N<sub>0</sub> (blue) and C/N<sub>0</sub>>20dBHz +valid ephemeris period (red) for PRN 3 along the day**

The red curve shows the period where the received signal incoming from PRN3 has a C/N<sub>0</sub> larger than 20dBHz and valid demodulated ephemeris with a 27dBHz DDT. As shown on figure 5, long periods without the possibility to demodulate the data are expected, and as a consequence, the ephemeris data exceed their 4hours validity period. So, we cannot use those satellites to compute the GEO position, even if the received signal is above 20 dBHz. Thus, we would like to ease the demodulation of the data.

Another important characteristic of the signals received in the geostationary environment is their Doppler frequency values. Indeed, the velocity of the GEO is around 4km/s in the Earth Centred Inertial coordinate system, and then, the rate of change in the distance between the GEO satellite and the GPS satellite can reach very important figure in some configurations, faster than for an earth user. So, the Doppler frequency for a GEO satellite ranges from +/- 15kHz, which is 3 times higher than for an earth user. When using GPS satellite with C/N<sub>0</sub>>20 dBHz, this figure falls down to +/-13kHz, nevertheless this figure

remains high and it implies too many operations during the acquisition process if the receiver has to cover this range.

The Dilution of Precision factors are not good in the geostationary case because the GPS satellite the GEO satellite sees are not numerous and they are not uniformly distributed in the space, they are inside a cone of 40° half-angle. By processing satellites with a C/N<sub>0</sub>>20dBHz, the receiver can use more satellites, and yet the PDOP factor remain higher than 10 for the GEO receiver. It implies a degradation of the position accuracy.

Finally, the main challenges encountered to design an autonomous and low cost GEO receiver are:

- The width of the doppler range which requires to predict the doppler. By roughly predicting the doppler, it enables the receiver to explore a reduced doppler range. This method reduces the processing cost (in term of energy consumption and processing time), as the remaining doppler uncertainty must be far lower than the initial +/- 15kHz global doppler range.
- The short and spaced period to demodulate the navigation data and especially the ephemeris and clock correction data: the ephemeris previously demodulated may lose their validity because of the inability of the receiver to update the last demodulated ephemeris. Thus, it is no more possible to compute the GEO position. To prevent from this problem, lowering the usual data demodulation threshold is investigated in the next section.

The next section presents the solution to face these problems and the strategy for the autonomous and low cost receiver.

## AUTONOMOUS RECEIVER STRATEGY

As already mentioned, the aim of this paper is to present an autonomous receiver which does not use "aided data" downloaded from Earth to compute its position. The complexity and the electric consumption of the receiver must be as low as possible.

The geostationary receiver position is computed along the day through an acquisition snapshot process. In the strategy, the position is not obtained with tracking loop only as in a classic receiver, notably to reduce the processing. The tracking loop channels used to demodulate the ephemeris and the almanacs are yet used to provide extra pseudorange measurements while they are functioning.

To reduce the energy consumption and the processing time, we must first reduce the doppler range. Indeed, the uncertainty on the Doppler frequency has a direct impact on the acquisition computation complexity. The number of Doppler bins to explore during the acquisition process

depends on the Doppler uncertainty which is the deviation between the true Doppler and the predicted doppler. With the unreduced Doppler uncertainty mentioned in the previous section ( $\pm 15\text{kHz}$ ), the calculation would be too expensive in terms of time and energy consumption. So, we need to reduce the Doppler uncertainty. One interesting solution to reduce the Doppler uncertainty is to know the almanacs or even better all the ephemeris data of the visible satellites. So, we consider that at least valid almanacs (not older than 1 week) are stored in the memory of the receiver:

- Cold Start

If it is the first ever start of the receiver, we consider that almanacs have been loaded before the geostationary satellite launching.

If the receiver has already worked in live conditions, the receiver uses the almanacs data which have been demodulated during this last processing. To remain valid, the almanacs should not be older than 1 week, so the receiver should not be shut down for more than a week.

- Warm Start

The receiver uses the current valid almanacs demodulated during the last 24 hours. It is always possible to demodulate the almanacs for the whole GPS constellation within one day. Indeed, to get it, the receiver must be able to demodulate the data over 12.5 minutes, which is the duration of the entire almanacs data. This process is done thanks to a tracking loop channel. It is only required to demodulate a set of almanac once a week. So the receiver needs just one tracking channel continuously operating for 12.5 minutes in a week to achieve the demodulation of the almanacs. As depicted on figure 4 (left) and 5, it is possible to receive a strong signal with  $C/N_0 > 27\text{dBHz}$  for more than 12.5 minutes over one day. So, the almanac demodulation is achievable with only one tracking channel and an almanac demodulation process must be launched at least once a week. It is the minimum requirement. A better recommendation would be to demodulate the almanacs once a day to improve their accuracy.

Knowing the almanacs data and so an approximate position of the GPS satellites, the remaining Doppler uncertainty only depends on:

- the uncertainty on the GEO receiver position set to 100km
- the time uncertainty between the receiver time and the GPS time set to  $\pm 3\text{seconds}$
- the uncertainty the local oscillator drift (we assume a 1 p.p.m oscillator grade).

The Doppler uncertainty falls down to only  $\pm 2000\text{Hz}$  with these assumptions, and it can be even lowered by a reduction of the local oscillator drift once the first Pseudorange is computed. With such a doppler uncertainty, the number of doppler bins to search during the acquisition process are reduced and so, the number of operations decreases too. Then, the computation time and the energy consumption are well reduced.

To be autonomous, the receiver must be able to compute the accurate position of at least four GPS satellites at each epoch. The accurate GPS positions are obtained thanks to the demodulated ephemeris. As shown in the previous section, for each PRN, long periods with signal power under the classic data demodulation threshold prevent from having continuously valid ephemeris. A solution is to decrease the data demodulation threshold, so that the period the receiver is able to demodulate the data will increase. As a consequence, the periods between two ephemeris demodulations will be shortened and we can expect we come close to a continuous availability of the ephemeris along a day. So, in the developed method, the data demodulation technique does not differ from a classic technique, but as the receiver try to demodulate data with a low power, then the BER may increase. The data demodulation threshold depends on the probability of bit error we accept during the processing of the data. the classic DDT is 27 dBHz which corresponds to a BER of  $6 \cdot 10^{-6}$ . As shown in [2], a DDT set to 25dBHz (BER of  $2 \cdot 10^{-4}$ ) is a good trade off between the number of satellites we can use to compute a position with valid ephemeris and the probability to demodulate the entire ephemeris data with no error.

Figure 6 shows the number of visible PRN with valid ephemeris and  $C/N_0 > 20$  by using a 25 dBHz data demodulation threshold for the Artemis geostationary satellite.

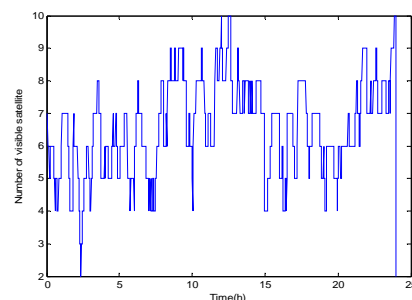


**Figure 6: Number of visible PRN with valid ephemeris and  $C/N_0 > 20$  and DDT=25dBHz**

There is only a short period where the GEO cannot use 4 satellites with valid ephemeris to compute its position. These periods only last 11 minutes with only 2 or 3 GPS satellites available. The average number of useable satellite is 6.6 with DDT=25 dBHz.

In conclusion, to ensure the GPS receiver is autonomous, the acquisition method which is implemented in the GEO receiver has to work at least down to 20 dBHz with the Data Demodulation Threshold equals to 25 dBHz.

Moreover, to reduce the number of operations carried out by the receiver during a day, it is possible to use the fact that the path of the geostationary satellite is predictable with a good accuracy. The almanacs give the position of

the GPS satellites with less than 1km error. The position of the geostationary satellite is known with a weak error. If it is the first start of the receiver, it is assume the GEO position is known with an error below 100km (the Kepler parameters loaded before launching the satellite can achieve this performance). If the receiver is running, the receiver uses the last calculated position whose error is less than 1 km (see the last section).

Knowing the GPS almanacs and the approximate position of the GEO, it is possible to foresee the elevation of the GPS satellites with regards to the GEO satellites. As the C/No is a function of the elevation angle as depicted by figure 2, the receiver is able to foresee the C/No signals of the different PRN.

The prediction can be made for several hours. Once a GEO position/velocity is calculated for a given epoch, its position can be accurately propagated with a simple force model, as the residual uncertainty on the GPS satellites position and the GEO propagated position does not affect significantly the accuracy of the elevation computation.

For the strategy presented in this paper, the acquisition snapshot process happens every 30 seconds. Then, the propagation of the GEO position is updated from each new calculated position, i.e every 30 sec. The propagation module works as shown on figure 7, with a GEO satellite position propagation time of 2 hours for example.

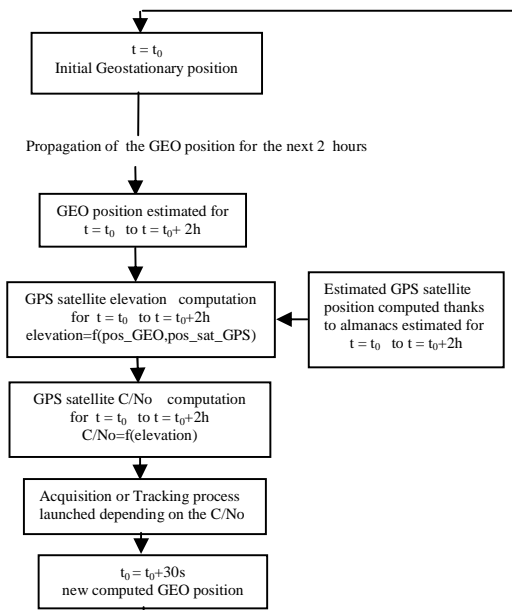


Figure 7: C/No prediction module

The main advantages of such a strategy are the following:

- the receiver only acquire PRN with a predicted C/No > 20 dBHz. As a consequence, it reduces the number of acquisition channel simultaneously working and the number of operations done.
- the receiver begins tracking signal only when the signal is strong. It reduced the risk of loss of lock.

The number of coherent (C) and non coherent (NC) integration are defined to achieve a given probability of detection for a given C/No. The knowledge of the C/No allow the receiver to chose the optimum C and NC for the next acquisition process of the satellite as the receiver knows the C/No of the signal. Thus, the number of operation is optimised. With such a principle, no acquisition or tracking will be achieved for nothing, i.e with signal power too weak to be processed successfully. Furthermore, it is possible to determine the number of operations the GEO receiver will achieve over one day for acquiring the GPS satellites by determining the C/No of every received signal as a function of the time.

The current set up strategy cope with an autonomous receiver and it allow to reduce the number of acquisition/tracking process to its minimum, and so to reduce the number of operation carried out.

The next section shows the acquisition algorithm used to compute the GEO satellite position.

## AUTONOMOUS ACQUISITION ALGORITHM AND RESULTS

In this section, the three acquisition methods used to compute the GEO satellite receiver position are briefly presented. They have already been presented in [2].

### 1+1ms FFT acquisition method

The structure of the acquisition loop is presented in figure 8. We assume that the signal has already been filtered by the RF front end filter and down-converted to the intermediate frequency  $f_I$ .

When it enters the acquisition loop, the signal has the following expression

$$s_f(kT_e) = Ad(kT_e - \tau)c_f(kT_e - \tau)\cos(2\pi f_I kT_e - \theta(kT_e)) + n(kT_e)$$

with

- $d$  : data transmitted trough the received GPS signal.
- $c_f$  : the filtered received spreading code.
- $\tau$  : group propagation delay.
- $\theta$  : received phase shift.
- $n$  : white Gaussian thermal noise with PSD  $N_0/2$  dB W Hz<sup>-1</sup>.

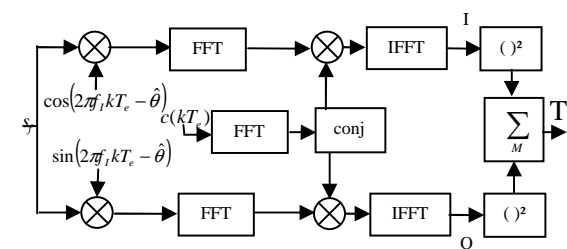


Figure 8: Acquisition loop structure

The principle of the acquisition depicted in figure 8 is as follows: once  $T_p$  seconds of the signal have been correlated in the FFT correlator, it is squared, and then the magnitude is stored into memory. Another  $T_p$  seconds of signal enters the loop and is processed as previously described. The magnitude is added to the previous result. This process is repeated  $M$  times,  $M$  being the non-coherent integration parameter. The whole process is repeated for each Doppler bin. The result of the processing is the classic acquisition matrix  $T$ . The maximum of the acquisition matrix gives the right [delay – Doppler] of the received signal. Let  $F_d$  be the Doppler uncertainty,  $\Delta f$  be the size of the Doppler bins (Hz) and  $N_{fd}$  the number of Doppler bins.

$$N_{fd} = \frac{F_d}{\Delta f} \text{ with } \Delta f = \frac{1}{2T_p}$$

The size along the code delay dimension depends on the sampling frequency the receiver uses. In this study, the sampling frequency is  $2fc$ . This values implies less processing but a lower resolution in the estimated delay. The size of the  $T$  matrix is then:

$$N_{fd} \times 2046 = 2T_p \cdot F_d \times 2046$$

Consequently, the number of operations are straight away linked to  $F_d$  and  $T_p$ .

The minimum  $T_p$  value is 1ms. The process used in our algorithm differs a bit from the one described in figure 9. With  $T_p=1\text{ms}$ , the FFT correlation is made on 2ms of signal with 2ms of local code as shown in figure9:

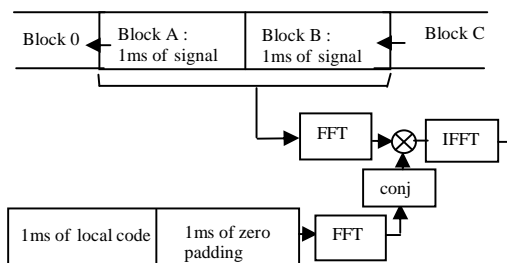


**Figure 9: 1+1ms FFT correlation process**

The incoming signal samples are put into a 2 ms data buffer, half of which will be replaced in a first-in first-out manner every 1 ms. The FFT of the incoming signal samples over 2 ms is taken. The extended local code replica is formed by appending 1 ms of zeros after the 1 ms of local code. The complex conjugate of the FFT of the extended replica is then computed.

The next correlation process will be carried out with block B and block C which is the millisecond coming after the block B.

This technique avoids the correlation losses that can happen if a bit transition data occurs inside the block A. Thanks to the 1ms zero padding, the FFT correlation over 2ms is not affected by the data bit transition. The switch

in the sign of the samples within block A after the bit transition and block B is compensated by the way the FFT correlation works.

### Half Bit acquisition method

The second acquisition method we investigate is the half bit method which is developed in [3]. The basic idea is to get rid of the losses due to a data bit transition occurring during a coherent summation of the signal by performing summation over time intervals which are not affected by a data bit transition. The principle of this method is to use 10 ms coherent integration time and to try two different intervals. The second interval is delayed by 10 milliseconds from the first. The acquisition process is the same as in the first acquisition method for each of the two sets corresponding to the two different intervals. As a consequence, for each set, the size of the  $T$  matrix depends of the parameter in the same manner as it is describes in the previous method.

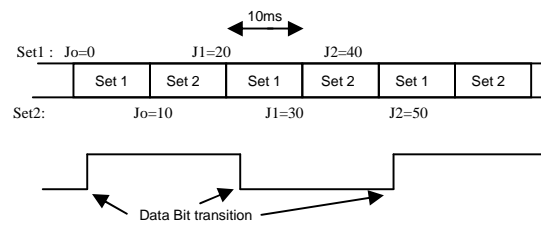


**Figure 10: Construction of the 2 sets**

With this temporal cut out, we are sure that at least one of the two intervals does not contain a data bit transition because transitions are separated by multiples of 20 milliseconds, the duration of a data bit. Thus, one of the two sets does not undergo losses due to a data bit transition. Moreover, the receiver does not need any knowledge about the data bit transition time. As long as the synchro bit is not carried out, the acquisition process could face important losses due to coherent integration over a data bit transition time. Thanks to this method, one of the set is guaranteed to have no bit transitions in any of its presquaring summation intervals.

Obviously, since this method processes an acquisition scheme over two sets of signals, the computational cost is more important than with the first method. The calculation is done over more than twice more signal length than with the first method.

### Double Block Zero Padding Method

Whereas the first two acquisition methods described in this section compute the classic acquisition matrix in order to find the right delay and the right Doppler frequency which affect the signal, in this method, the delay-doppler research is not achieved following that kind of time-frequency research with the double block zero padding algorithm. The method is described in [4], [5], [6], [7].



The approach to achieve signal acquisition here is to split N milliseconds of data sample into M blocks. Then, partial correlations (i.e on less than 1ms of signal) on the M blocks are made to find the delay and the Doppler. The number of operation to achieve this acquisition scheme is far less than the two other processing methods. The performances of the three acquisition methods described in this section are evaluated in the next subsection for a geostationary orbit, notably the position error is computed thanks to a least square algorithm.

### Acquisition results

The simulations are conducted over 24 hours. The GPS signals are simulated under MATLAB.

The simulated data carry the characteristics the GPS signals should have if they were processed by a real receiver on a geostationary orbit. For each epoch, the elevations of the GPS satellites as well as their distances with the GEO satellite are used to compute the C/No of the signals reaching the receiver. The Doppler and the transmission delay are also obtained by simulating the GEO orbit and the GPS satellites orbits.

The lowest acceptable signal strength to process the GPS signals is set to 20 dBHz. With a predicted C/No under that threshold, we will not try to acquire the corresponding satellite.

The acquisition of all visible PRN with valid ephemeris and with a C/No>20 dBHz is performed every 30 seconds during the 24 hours of simulation. At each epoch, thanks to the delay measured by the acquisition process the estimated position of the user is computed as well as the positioning error.

To achieve the performances described after, the duration of the signal can be as long as 3 seconds.

Depending on the C/No the receiver should get the signal coming from a PRN, we define the number of coherent and non-coherent integration carried on during the acquisition process for the first two method. We remind that the double block zero padding method does not use coherent nor non-coherent integration.

- 1+1ms FFT acquisition method

Signal strength	Coherent acquisition (ms)	Non-Coherent acquisition	Signal Duration (s)
C/No>30	1	100	0.1
30>C/No>26.5	1	200	0.2
26.5>C/No>24	5	200	1
24>C/No>22	10	150	1.5
C/No<22	10	250	2.5

- Half Bit acquisition method

Signal strength	Coherent acquisition (ms)	Non-Coherent acquisition	Total Signal Duration (s)/ Signal set duration
C/No>30	10	20	0.2/0.1
30>C/No>26.5	10	40	0.4/0.2
26.5>C/No>24	10	150	1.5/0.75
24>C/No>22	10	250	2.5/1.25
C/No<22	10	350	3.5/1.75

- Double Block Zero Padding Method

Signal strength	Signal Duration (ms)
C/No>30	100
30>C/No>26	500
26>C/No>22	1000
C/No<22	1500

For each epoch, the three algorithms compute the code delay for each visible satellite (with C/NO>20 dBHz) with valid ephemeris data. With these information, the pseudorange measurements are computed. We can compute them because we make the assumption that the GEO position is known with the uncertainty of less than 300km (which is the distance covered by 1ms of signal). Since the GEO satellite is on orbit and that orbit does not fluctuate fast, we consider our assumption to be realistic. The computed delays represent the estimated position within a 300km uncertainty.

The GEO position is estimated thanks to a classic Least Square method.

The geostationary orbit simulated is the Artemis (PRN124) orbit.

The mean position errors are summed up in the following table for the three different acquisition method.

	1 +1 ms method	Half Bit method	Double Block Zero Padding method
Along track Error (m)	101.1	102.4	211
Radial track Error (m)	742	745	1659
Tangent track Error (m)	67.8	69.3	136
Geometric error (m)	751	755	1677
time proportion with more than 4 satellites acquired successfully	97%	96.8%	88%

### Mean position error for the three acquisition methods

The error is much more significant along the radial track This is due to the configuration of the GPS satellites. They are all usually located in front of the GEO satellite, inside a little area, so that the accuracy of the measurements is not good along the radial track. The different GPS satellites do not provide enough

information to compute a position with a good accuracy along this axis.

The results are similar with the Half Bit method and the 1+1ms method. Due to the delay resolution, the mean error is covariance 150 geometric error

### Peak extrapolation technique

The previous results are obtained by computing the position thanks to a classic Least Square method. However, we must stress the fact that the accuracy on the code delay is only  $\frac{1}{2}$  chip as the sampling frequency is taken to  $2f_c$ , where  $f_c$  is the code frequency. Thus, the accuracy on the estimated pseudorange for each satellite cannot be better than 150 meters (length of  $\frac{1}{2}$  chip). Combined with the poor DOP value for the GEO receiver, it explains the low accuracy concerning the GEO satellite positioning.

To achieve a better positioning, a simple extrapolation technique is used. The aim is to improve the accuracy of the code delay estimation. It is based on the extrapolation of the acquisition matrix.

It assumes that the autocorrelation function of the code is a perfect triangle with opposite slope on both side of the peak. Once the maximum  $(\hat{\tau}, F\hat{d})$  of the acquisition matrix is located, the algorithm applies that property to extrapolate the location of the peak as shown on figure 11.

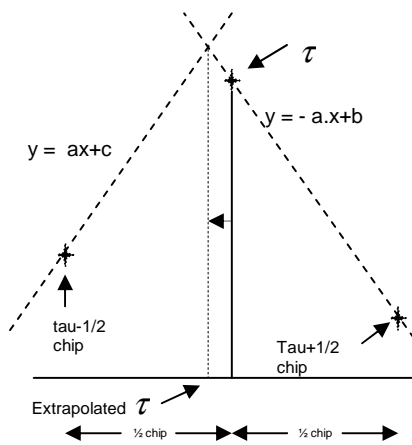


Figure 11: Extrapolation of the estimated code delay  $\tau$

The amplitude of the sample after the peak and before the peak is compared. The sample with the lowest amplitude indicates that the slope (in absolute value) between the peak and this sample is the highest (-a in figure 11). A straight line with the slope +a is drawn passing by the sample with the highest amplitude. The intersection between the two straight lines gives the extrapolated Tau. This simple extrapolation technique provides an average good improvement in the accuracy of the estimated Tau and then, a good improvement in the accuracy of the GEO position.

The extrapolation technique cannot work with the Double Block Zero Padding method as it does not use the classic acquisition matrix to find the right delay-doppler.

Position error with satellites with valid ephemeris (improvement compared without extrapolation)	1+1ms method	Half Bit Method
Along track Error (m)	68 (32%)	62 (39%)
Radial track Error (m)	539 (27%)	465 (37.5%)
Tangent track Error (m)	37 (44%)	39.9 (42%)
Geometric error (m)	544 (27.5%)	470.8 (37.7%)

### Position error with peak extrapolation technique

The comparison shows the improvement thanks to this simple extrapolation. The position accuracy increases by 30 to 45% compared to positions computed with the initial measurements. However, the positioning error remains high in spite of the improvement leads by the extrapolation technique. In order to improve the positioning accuracy, an orbital filter is developed to be implemented within a Kalman Filter in the next section.

### ORBIT DETERMINATION WITH A KALMAN FILTER

The motion of the geostationary satellite can be described by all the forces applying on him. Indeed, thanks to the 3<sup>rd</sup> Newton law, linking the acceleration to the forces applying to the satellite, it is possible to accurately calculate the position and the velocity of the satellite. The accuracy of the computed position depends on the force model complexity. For a geostationary satellite, the main force is the earth gravitational attraction. But other perturbing forces drive the movement of GEO satellite too. They are listed in the next table with their order of magnitude of the associated acceleration in  $m.s^{-2}$ .

Force	Related acceleration magnitude ( $m.s^{-2}$ )
spherically symmetric earth's gravity	0.22
Non spherical part of earth's gravitational potential	$10^{-6}$
Attractions due to sun, moon /Other planet	$10^{-5}$ / $10^{-9}$
Solar radiation pressure	$10^{-7}$
solar corpuscular wind	$10^{-10}$
orbit maneuvers	$10^{-3}$
satellite attitude control maneuvers	$10^{-10}$

### Acceleration magnitude of the forces driving the GEO motion

Most of the forces have natural origin and most of them can be analytically predicted. The forces created by the satellite ground control in attempting to manipulate its position and orientation in space are punctual and they are taken into account.

Due to the non spherical symmetric earth, the earth gravity is decomposed into spherically symmetric earth's gravity potential P1 and the non spherically part of earth's gravitational potential P2. The earth gravity potential is:

$$U(r, \lambda, \varphi) = \frac{GM}{r} + GM \sum_{l=2}^{\infty} \sum_{m=0}^l \frac{R^l}{r^{l+1}} P_{l,m}(\sin(\varphi)) [C_{l,m} \cos(m\lambda) + S_{l,m} \sin(m\lambda)]$$

$$= P1 + P2$$

where  $P_{l,m}$  are the Legendre functions of degree l and order m.  $r$ ,  $\varphi$  and  $\lambda$  are, respectively the geocentric distance, latitude, and longitude of the GEO satellite.  $C_{l,m}$  and  $S_{l,m}$  are harmonics coefficients of the earth potential of degree l and order m. The acceleration of the satellite is the gradient of the potential function U. In this study, the earth gravity potential is limited to:

$$U(r, \lambda, \varphi) = \frac{GM}{r} + GM \frac{R^2}{r^3} P_{2,0}(\sin(\varphi)) C_{2,0}$$

The influence of the other term in P2 are negligible compared to the retained term with  $C_{2,0}$ .

The moon and sun gravity force depends on the sun and moon position with regards to the geostationary satellite. Their positions are calculated thanks to the algorithm described in [9]. It just requires the GPS time. The corresponding acceleration is calculated by:

$$\vec{a}_{moon} = GM_{moon} \left( \frac{\vec{SM}}{|\vec{SM}|^3} - \frac{\vec{OM}}{|\vec{OM}|^3} \right) \quad \vec{a}_{sun} = GM_{sun} \left( \frac{\vec{SSun}}{|\vec{SSun}|^3} - \frac{\vec{OSun}}{|\vec{OSun}|^3} \right)$$

Where  $\vec{SM} / \vec{SSun}$  is the satellite to Moon/Sun vector and  $\vec{OM} / \vec{OSun}$  is the earth gravity centre to Moon/Sun vector.

The tidal acceleration due to the sun and moon is not taken into account as well as the force due to the other planet. The solar radiation pressure and the solar corpuscular wind are not used to compute the satellite motion in this study. Finally, only the first three forces of the previous table are used to compute the satellite equation motion and the total acceleration is:

$$\vec{a}_{tot} = -grad(U) + \vec{a}_{sun} + \vec{a}_{moon}$$

This equation of the GEO satellite motion is used as the state propagation model of the Kalman filter. As it is non linear an extended Kalman filter (EKF) solution is implemented. The role of this filter is to provide estimates of the position and velocity of the GEO using GPS pseudorange measurements.

This filter is described below:

- The state vector is defined as  $X = [\dot{x}, \dot{y}, \dot{z}, x, y, z, b, cd]$ , where  $\dot{x}, \dot{y}, \dot{z}, x, y, z$  are the GEO satellite velocity and position in the Earth Centred

Inertial frame, and  $b, cd$  are the GEO satellite clock bias and drift.

- The state transition equation,  $X_{k+1} = f(X_k) + W_k$  is not linear as the acceleration depends on both x, y and z. The transition state equation of the EKF is obtained by linearization and discretization of the GEO satellite motion equation.

$$\begin{aligned} \dot{x}(k) &= \dot{x}(k-1) + a_{x_{sat}}(x, y, z)T + w_x \\ \dot{y}(k) &= \dot{y}(k-1) + a_{y_{sat}}(x, y, z)T + w_y \\ \dot{z}(k) &= \dot{z}(k-1) + a_{z_{sat}}(x, y, z)T + w_z \\ x(k) &= x(k-1) + \dot{x}(k-1)T + w_x \\ y(k) &= y(k-1) + \dot{y}(k-1)T + w_y \\ z(k) &= z(k-1) + \dot{z}(k-1)T + w_z \\ b(k) &= b(k-1) + cd(k-1)T + w_b \\ cd(k) &= cd(k-1) + w_{cd} \end{aligned}$$

T is the time interval between two epochs of the EKF and the state noise vector  $w_k$  is normal distributed ( $w_k \sim N(0, Q_k)$ ).

- The relationship between observation vector Y and the state vector X at the instant n is:

$$Y_k = h(X_k) + V_k$$

with  $v_k \sim N(0, R_k)$ ,  $R_k$  being the measurement noise covariance matrix.

The size of the vector  $Y_k$  is equal to the number of processed GPS satellites at epoch k. Assuming the number of measurement is M,  $R_k$  is a  $M \times M$  matrix that consists in the estimates of the pseudorange error variance for each GPS satellite. It is a diagonal matrix, as each measurement is assumed to be independent with the others, with a constant value:  $\sigma_{Pseudorange}^2 = 150^2$ ; 150m standing for the remaining uncertainty on the pseudorange due to the uncertainty on the code-delay measurement ( $\frac{1}{2} chip$ ).

The expression of h for the i<sup>th</sup> satellite is given by:

$$h(x, y, z, b) = \sqrt{(x_{GPS}^i(k) - x(k))^2 + (y_{GPS}^i(k) - y(k))^2 + (z_{GPS}^i(k) - z(k))^2} - b(k)$$

Now let us remind the equations of the EKF:

$$\begin{cases} \hat{X}_{k+1|k+1} = \hat{X}_{k+1|k} + K_{k+1} [Y_{k+1} - h(\hat{X}_{k+1|k})] \\ \hat{X}_{k+1|k} = f(\hat{X}_{k|k}) \end{cases}$$

$$K_{k+1} = P_{k+1|k} H_{k+1}^T (H_{k+1} P_{k+1|k} H_{k+1}^T + R_{k+1})^{-1}$$

$$P_{k+1|k+1} = P_{k+1|k} - K_{k+1} H_{k+1} P_{k+1|k}$$

$$P_{k+1|k} = F_k P_{k|k} F_k^T + Q_k \quad (1)$$

$$F_k = \left. \frac{\partial f(X_k)}{\partial X_k} \right|_{X_k = \hat{X}_{k|k}} \quad \text{and} \quad H_{k+1} = \left. \frac{\partial h(X_{k+1})}{\partial X_{k+1}} \right|_{X_{k+1} = \hat{X}_{k+1|k}}$$

$P_{k+1|k+1}$  and  $P_{k+1k}$  are respectively the a posteriori and a priori covariance of the Kalman filter. The a posteriori covariance gives the uncertainty in the determination of the satellite orbit.  $P_0$ , the initial covariance matrix, is an 8x8 diagonal matrix with  $P_{0,vel}$  the first three elements of the diagonal,  $P_{0,pos}$  the next three and  $P_{0,cl}$  the last two.

$K_{k+1}$  is the gain of the Kalman filter.

The state noise covariance matrix  $Q$  models the effects of both linearization, discretisation error and unmodeled dynamics. Here,  $Q$  is a 8x8 matrix.

$$Q = \begin{pmatrix} Q_{vel1,1} & 0 & . & . & . & . & . & . & 0 \\ 0 & Q_{vel2,2} & 0 & . & . & . & . & . & . \\ . & 0 & Q_{vel3,3} & 0 & . & . & . & . & . \\ . & . & 0 & Q_{pos1,1} & 0 & . & . & . & . \\ . & . & . & 0 & Q_{pos2,2} & 0 & . & . & . \\ . & . & . & . & 0 & Q_{pos3,3} & 0 & 0 & . \\ . & . & . & . & . & 0 & Q_{7,7} & Q_{7,8} & . \\ 0 & . & . & . & . & . & 0 & Q_{8,7} & Q_{8,8} \end{pmatrix}$$

$Q_{pos}$  and  $Q_{vel}$  are constant.  $Q_{7,7}, \dots, Q_{8,8}$  depends on the type of the receiver clock. It is assumed that the oscillator of the receiver is an OCXO. The covariance for the clock receiver is then computed thanks to the Allan variance with classic OCXO parameter.

The next table illustrates the figures used to initialize the Kalman filter in our implementation.

$Q_{vel}$	$0.01^2 \text{ (m/s)}^2$
$Q_{pos}$	$1^2 \text{ (m)}^2$
$Q_{7,7} \quad Q_{7,8} \quad Q_{8,7} \quad Q_{8,8}$	$1.07 \quad 0.037 \quad 0.037 \quad 0.107$ $\text{(m)}^2$
$P_{0,vel}$	$2^2 \text{ (m/s)}^2$
$P_{0,pos}$	$200^2 \text{ (km/s)}^2$
$P_{0,cl}$	$0.1 \text{ (m)}^2$

**Kalman filter parameter**

Finally, the functioning of the Kalman filter is depicted on figure12:

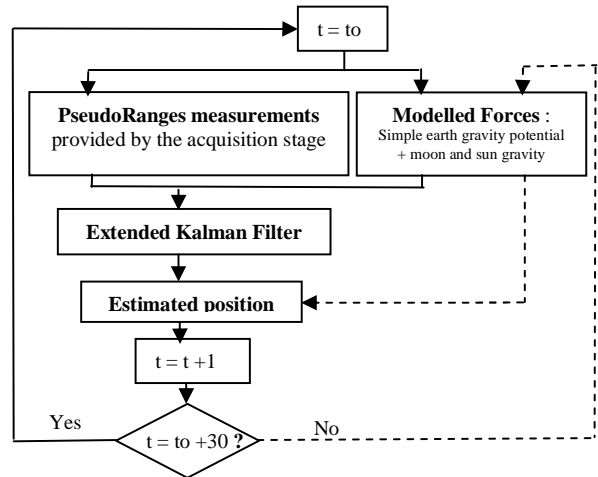


**Figure 12: Kalman Filter functioning**

It is assumed that pseudoranges measurements are available only every 30 seconds: the duration between two Kalman filter state vector estimates updates is then 30s. Between these epochs, every second, the estimated position is propagated thanks to the modelised forces only. The linearised satellite motion equation is used to compute the transition state equation of the Kalman filter and to propagate the position between two Kalman filter epochs

### Kalman Filter Results

The observations correspond to the pseudoranges calculated at the output of the acquisition process. The acquisition process supply pseudoranges every 30 seconds in our strategy. Thus, the epoch of the Kalman filter are spaced by 30 seconds too. However, it is possible to propagate the position of the GEO satellite during this 30s interval with the orbital filter, i.e to use only the state transition equation to propagate the GEO position between two GPS measurements. In this case, the covariance matrix has to be propagated between two 30s-spaced epochs to express the position and velocity derivation due to the orbital filter. It is propagated as in equation (1). The position error and the velocity error are given in figure 13 and figure14.

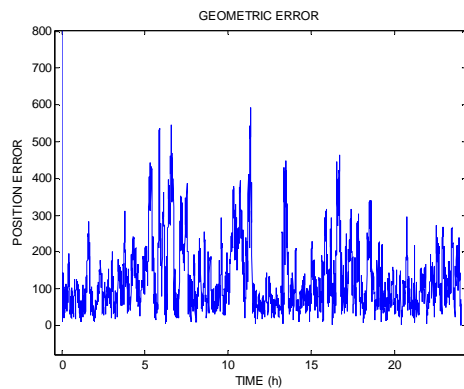


**Figure 13: Geometric position error with the Kalman filter**

The mean error significantly decreases with the Kalman filtering. It falls down to 125.1 m. Compared to the 750m error with the acquisition snapshot only (for method 1 and method 2) and 450 to 550 m error obtained with the peak extrapolation technique, the improvement provided here is really interesting. Even with an initial error of 50km on each axis, the kalman filter converges at the first iteration.

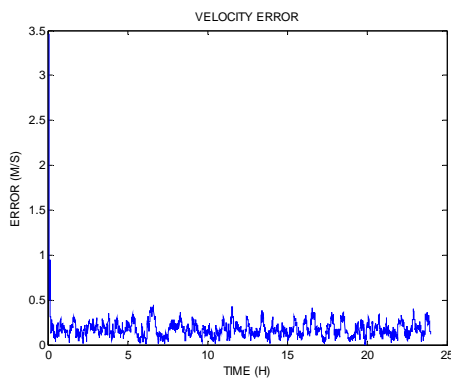


**Figure 14: Velocity error with the Kalman filter**

Besides, the mean velocity error is only of 0.17m/s with the Kalman filter.

The use of the Kalman filter enables us to overcome the problem due to the high PDOP value which degraded the position measurements obtained only thanks to acquisition snapshot process.

**Computational Cost Over one Day**

Last in this section we illustrate the computational cost of our strategy.

The computational cost is estimated for the three acquisition techniques. It also includes the number of operations carried out to produce a position thanks to the Kalman filter. Using the C/NO prediction module, the computational cost of the three different acquisition methods is computed by taking into account the expected C/No of the received signal along the day for every satellite and the corresponding coherent acquisition

duration and number of non coherent integration. For a given epoch, the receiver tries to acquire only useful satellites and their C/No are predicted. Thus, the number of operation carried out by the receiver at each epoch can be estimated which leads to the total number of operations carried out over one day.

	1+1 ms FFT method	Half Bit Method	DBZP method	Kalman Filter
Number of multiplication	$5.75 \cdot 10^{14}$	$4.86 \cdot 10^{14}$	$2.49 \cdot 10^{12}$	$1.05 \cdot 10^8$
Number of application	$3.47 \cdot 10^{14}$	$2.92 \cdot 10^{14}$	$1.24 \cdot 10^{12}$	$1.35 \cdot 10^8$

**Number of operations carried out for one day of positioning**

The number of operations related to the Kalman filter plays a little part in the total amount of operation.

The first two methods show similar amount of operation. Whereas the Half Bit method uses two sets of data and as a consequence, a longer signal duration needed for processing than with the 1+1ms FFT method, the number of operations are not more numerous. In fact, in the first method, each 1ms correlation operation are done with 2ms of signal. Thus, the FFT operations are calculated over twice the number of points it is done with the Half Bit method. Moreover, the signal duration of one set of data in the Haf Bit method is shorter than for the 1+1ms FFT method (Table1). It explains the higher number of operation for the first method compared to the second one. As expected, the number of operation carried out with the DBZP is 100 times lower than the two other methods. The signal duration used is shorter and this method does not try different local Doppler compensation as it is done when computing the matrix acquisition with the first two methods. However, the position error is well higher.

**CONCLUSION**

A method to provide autonomous positioning for geostationary satellite has been presented in this study. To provide continuous positioning with no outage, we propose to lower the Data Demodulation Threshold down to 25dBHz. A mean to reduce the number of operations carried out by the receiver and so to reduce the energy consumption is done thanks to a C/No prediction module. In this study, the GEO satellite position is obtained thanks to acquisition snapshot once every 30 seconds. Between two snapshots, the receiver does not work, except if a tracking process is used to demodulate ephemeris or almanacs: this also allows reducing the energy consumption. Three acquisition techniques are embraced in this study: they provide positioning with large error even with a peak acquisition extrapolation technique. This is due to the high PDOP values and the pseudorange resolution at the output of the acquisition process. To

improve the accuracy of the positioning, a Kalman Filter is implemented. A simple force model is used to compute the state transition model. The pseudo ranges measurements obtained with the acquisition process are used as the observations of the filter. Between two GPS measurements (30 seconds), the position of the GEO satellite is propagated using the simple forces model only. With this principle, the GEO positioning mean error is significantly reduced and it falls down to 125 meters. Last, the number of operations to achieve the acquisition process and the Kalman filter operations has been investigated. Thanks to the C/NO prediction module, the receiver can foresee the C/NO of the received signals. Thus, it can assess the length and the number of correlations it will do over a day. It is then possible to compute the total number of operations carried out by the receiver over a day to obtain the GEO position. A future work will be to convert this number of operation into a number of cycles for a given processor. This can lead to the total energy consumption required for the receiver to compute its position over a day.

## ACKNOWLEDGMENTS

The figure1 is extracted from a “GPS world” article. The article is entitled “Autonomous GPS Positioning at High Earth Orbit”, april2006. We thank the authors (W.Bamford, N Winternitz, C Hay)

## REFERENCES

- [1] **B.Chibout,C.Macabiau** *Investigation of new processing techniques for geostationary satellite positioning* **ION NTM 2006**
- [2] **B.Chibout,C.Macabiau** *Comparison of acquisition techniques for geostationary satellite positioning* **ION NTM 2007**
- [3] **M. Psiaki** *Block Acquisition of weak GPS signals in a software receiver* **ION GPS 2001**
- [4] **D. Lin, J.B.Y Tsui** *Direct P(Y)-Code Acquisition algorithm for software GPS receiver* **ION GPS 99**
- [5] **D. Lin, J.B.Y Tsui** *Comparison of acquisition methods for software receiver* **ION GPS 2000**
- [6] **D. Lin, J.B.Y Tsui** *A software GPS Receiver for weak Signals* **Proc IEEE MTT-SDigest May2001**
- [7] **N. Ziedan J.L. Garrison** *Unaided Acquisition of Weak GPS Signals Using Circular Correlation or Double-Block Zero Padding* **IEEE 2004**
- [8] **S.Gupta** *A Program to Compute the Coordinates of a Geostationary Satellite for Time and frequency broadcast* **IEEE Transactions On Instrumentation and Measurement, Vol. 42, No. 2, April 1993**